

Analysis of heat fluxes and their influences on vertical flame spread over PMMA walls by a large eddy simulation

Kazui Fukumoto¹, Changjien Wang¹, and Jennifer X Wen²

¹Hefei University of Technology
No.193, Tunxi Road, Hefei, 230009, Anhui, P.R.China

²University of Warwick

Coventry, CV4 7AL, United Kingdom

1 Introduction

Upward fire spreading scenario is of importance for fire safety engineering owing to its faster spreading rate than those of other scenarios. Some previous studies also discussed underlying heat transfer and reported the wall heat fluxes in the flame spread phenomena [e.g. 1–4]. Orloff et al. [1] suggested that a radiation contribution reached 75 to 80% of the total heat transfer above 76 cm. Singh and Gollner [3] experimentally investigated local heat fluxes on laminar boundary layers over methanol, ethanol and poly methyl methacrylate (PMMA). They found that the convective heat flux was nearly 85–90% of the total heat flux; on the other hand, a radiation contribution was relatively minor in the laminar boundary layers. Tsai [4] experimentally investigated an influence of a sample width on total heat flux. Total heat flux did not vary clearly, whereas faster flame spreading with flame height was observed with a wider flame. In spite of above progress, none of previous experimental and numerical studies reported the relative magnitudes of individual heat flux components and their influence on flame spread, for which insight is still lacking despite their significance as the driving force for flame spread. For instance, Ren et al. [5] evaluated convective and radiative heat fluxes on wall fire scenarios; however, these are considered different from flame spread scenarios. The present study is hence focused on a detailed analysis of individual heat flux components and their effect on flame spread. The radiative heat fluxes owing to soot and gases will be distinguished; the relative importance of radiative heat flux owing to soot on flame spread will be discussed.

2 Method

A LES based FireFOAM solver [6] is used as a basic numerical framework. The methodology was written in a previous study [7]; hence, modifications are explained following sections. The model parameters for the gas and solid phases were also presented in reference [7].

2.1 Combustion model and reaction mechanisms

In this study, Chen et al.'s eddy dissipation concept model [8] was applied; they successfully validated the model with several pool fire cases. The combustion model was further extended to consider laminar-turbulent transition and finite reaction rates in previous studies [7,9]. Pyrolysed PMMA is treated as methyl methacrylate with Tarrazo et al.'s irreversible single one-step chemistry model [10], which was validated with non-premixed and premixed flame scenarios.

2.2 Soot and radiation treatments

The soot model is adopted from the development of Wang et al. [11] in this study. Their validation studies with medium scale heptane and toluene pool fires achieved reasonably good agreement with the measurements. The smoke point height of $C_5H_8O_2$ was set to 0.105 following Tewarson's study [12]. For radiative heat transfer, the finite volume discrete ordinate method is used with the weighted sum of grey gases model (WSGGM) of Smith et al. [13] for gas emissivity. The soot absorption coefficient $a_{rad,soot}$ is calculated as $a_{rad,soot} = C_{soot} f_v T$ following a previous study [7].

2.3 Pyrolysis model for solid regions

The 1-D diffusion equation for sensible enthalpy with the Arrhenius type pyrolysis model suggested in a previous study [7] is solved, and a description is properly presented in a previous study [7]. Furthermore, Marinite was newly considered as an inert wall, giving realistic heat flux on it. The respective model parameters for a marinite wall are: density $\rho_{solid} = 800 \text{ kg/m}^3$ [14], heat conductivity $\lambda_{solid} = 0.1154 \text{ W/m/K}$ [14], heat capacity $Cp_{solid} = 1110 \text{ J/kg/K}$ [14], reflectivity $r_{rad,solid} = 0.02$ ($= 1 - \alpha_{rad,solid}$), absorptivity $\alpha_{rad,solid} = 0.98$ [3] and emissivity $\varepsilon_{rad,solid} = 0.98$. The model parameters for PMMA were presented in a previous study [7], whereas $\lambda_{inter} = \lambda_{gas}$ on a PMMA surface is used in order to keep consistency to estimate the convective heat flux between marinite and PMMA, where λ_{gas} is estimated by the modified Eucken equation [15].

3 Results

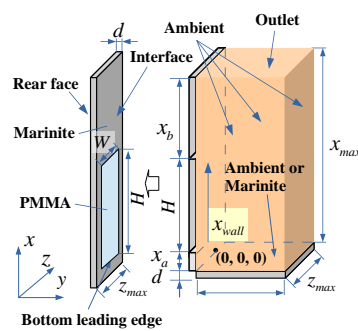


Figure 1 Computational domain

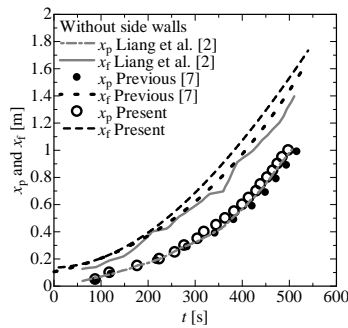


Figure 2 Pyrolysis (x_p) and flame (x_i) heights

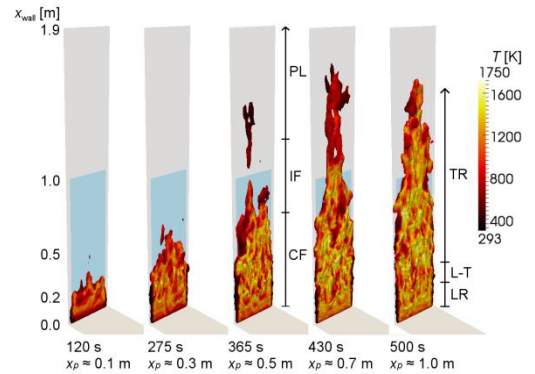


Figure 3 Flame spreading

The large scale flame spread test of Liang et al. [2] was simulated. The authors recently validated the predictions for the pyrolysis (x_p) and flame (x_i) heights, and total heat flux for this case [7]. The simulation has been conducted in the present study to take into account the non-combustible wall region and extract output for the individual heat fluxes. The specific dimensions in Fig. 1 are: $H = 1.0 \text{ m}$, $W = 0.304 \text{ m}$, $d =$ 27th ICDERS – July 28th - August 2nd, 2019 – Beijing, China

0.01 m, $x_{\max} = 1.9$ m, $y_{\max} = 0.7$ m, $z_{\max} = 0.36$ m, $x_a = 0.005$ m and $x_b = 0.895$ m. The first grid sizes from the wall were set to $\Delta y = 1$ mm, $\Delta x = 5$ mm and $\Delta z = 8$ mm; these grid sizes were considered sufficient because of a grid sensitivity study in a previous study [7]. In the solid region, the number of cells was set to 70 uniformly in the direction along the depth. The marine condition was set on the floor in Fig 1. A total of 1,197,000 cells for the gas region and 1,417,500 cells for the solid region were used. Ignition was triggered by imposing fixed radiative heat flux of 45 kW/m² for 75 s at $0.005 \leq x \leq 0.05$ m.

Figure 2 shows the pyrolysis and flame heights, where the pyrolysis front is defined as 580 K at 0.5 mm depth in the PMMA wall following a previous study [7]. The pyrolysis temperature must be specified for a comparison of flame spreading with the experimental data. The flame height x_f is estimated as $x_f = \max(x - x_a)$ when $\tilde{Y}_{fu} - \tilde{Y}_{O_2} / s \geq 0$, where $\max()$ indicates the maximum coordinate and s is the stoichiometric oxygen-fuel mass ratio, \tilde{Y} is the density weighted average mass fraction and fu is the fuel. The present predictions are close to the experimental data. The present x_p is closer than that of a previous simulation, whereas the previous x_f is slightly better than that of the present simulation.

Figure 3 shows iso-surfaces of flame volume defined by criterion $R_o = 1.0 / (1 + s \tilde{Y}_{fu} / \tilde{Y}_{O_2})$, where $0 \leq R_o \leq 0.99$, PL is the plume region, IF is the intermittent flame region, CF is the continuous flame region, LR is the laminar region, L-T is the laminar-turbulent transition region and TR is the turbulent flame region. The region's definitions can be found in a previous study [7].

Figure 4 shows the total heat flux (a); total and individual heat flux components, and their fractions when the pyrolysis height $x_p \approx 0.1$ (b), 0.5 (c) and 1.0 m (d), where q''_{conv} is the convective heat flux, q''_{rad} is the radiative heat flux, q''_{tot} is the total heat flux ($= q''_{conv} + q''_{rad}$), q''_{re} is the absolute value of re-radiative heat flux, and q''_{net} is the net heat flux ($= q''_{tot} - q''_{re}$). The heat fluxes were averaged for 10 second started from the respective times when pyrolysis occurred with the fixed mass flow rate to prevent further flame spread. q''_{rad} is divided into two components, i.e., (i) radiative heat flux owing to combustion gas $q''_{rad,gas}$ and (ii) that owing to soot $q''_{rad,soot} \cdot q''_{rad,gas}$ is obtained by a different simulation started with the same data but $C_{soot} = 0$ is used to remove $q''_{rad,soot}$ from q''_{rad} ; then $q''_{rad,soot}$ is given by $q''_{rad,soot} = q''_{rad} - q''_{rad,gas}$. As can be seen from Fig. 4 (a), the predicted q''_{tot} is similar to the experimental data of Tsai [18]. When $x_p \approx 0.1$, q''_{conv} / q''_{tot} is about 80%; q''_{rad} / q''_{tot} is about 20%. These are quantitatively in line with the measurements of Singh and Gollner [3]. According to a previous study [7], a laminar flame was seen at $x_{wall} < 0.18$ m; therefore, the entire region is considered laminar. q''_{tot} and q''_{conv} fall sharply with an increase in x_{wall} close to the bottom leading edge owing to relatively high gas temperature there; then a rate of decreasing slow down until $x_{wall}/x_p \approx 2$, and afterwards q''_{tot} , q''_{conv} and q''_{net} start to decrease rapidly after $x_{wall}/x_p \approx 1.6$. Evolution trends in the total and individual heat fluxes $x_p = 0.5-1.0$ m are found to be similar; i.e., q''_{tot} , q''_{conv} , q''_{re} and q''_{net} are reduced sharply near the bottom of the PMMA wall; the respective heat fluxes are relatively high the in CF region, these decrease near from the border of the CF-IF regions. It can also be observed from Fig. 4 that $q''_{rad,soot}$ rises as pyrolysis proceeds ($x_p = 0.1 \rightarrow 1.0$ m), resulting in an increase in q''_{rad} . At $x_{wall}/x_p \approx 1.0$ m, $q''_{conv} / q''_{tot} \approx 0.8$, and $q''_{rad} / q''_{tot} \approx 0.2$ when $x_p \approx 0.1$ m, $q''_{conv} / q''_{tot} \approx 0.6$ and $q''_{rad} / q''_{tot} \approx 0.4$ when $x_p \approx 0.5$ m, and $q''_{conv} / q''_{tot} \approx 0.4$ and $q''_{rad} / q''_{tot} \approx 0.6$ when $x_p \approx 1.0$ m.

Next, the wall fire scenario of Hebert et al. [16] was simulated; its dimensions in Fig. 1 are: $H = 0.4$ m, $W = 0.2$ m, $d = 0.03$ m, $x_{\max} = 0.96$ m, $y_{\max} = 0.25$ m, $z_{\max} = 0.248$ m, $x_a = 0.05$ m and $x_b = 0.51$ m. Grid creation and ignition procedures were the same as the scenario of Liang et al.

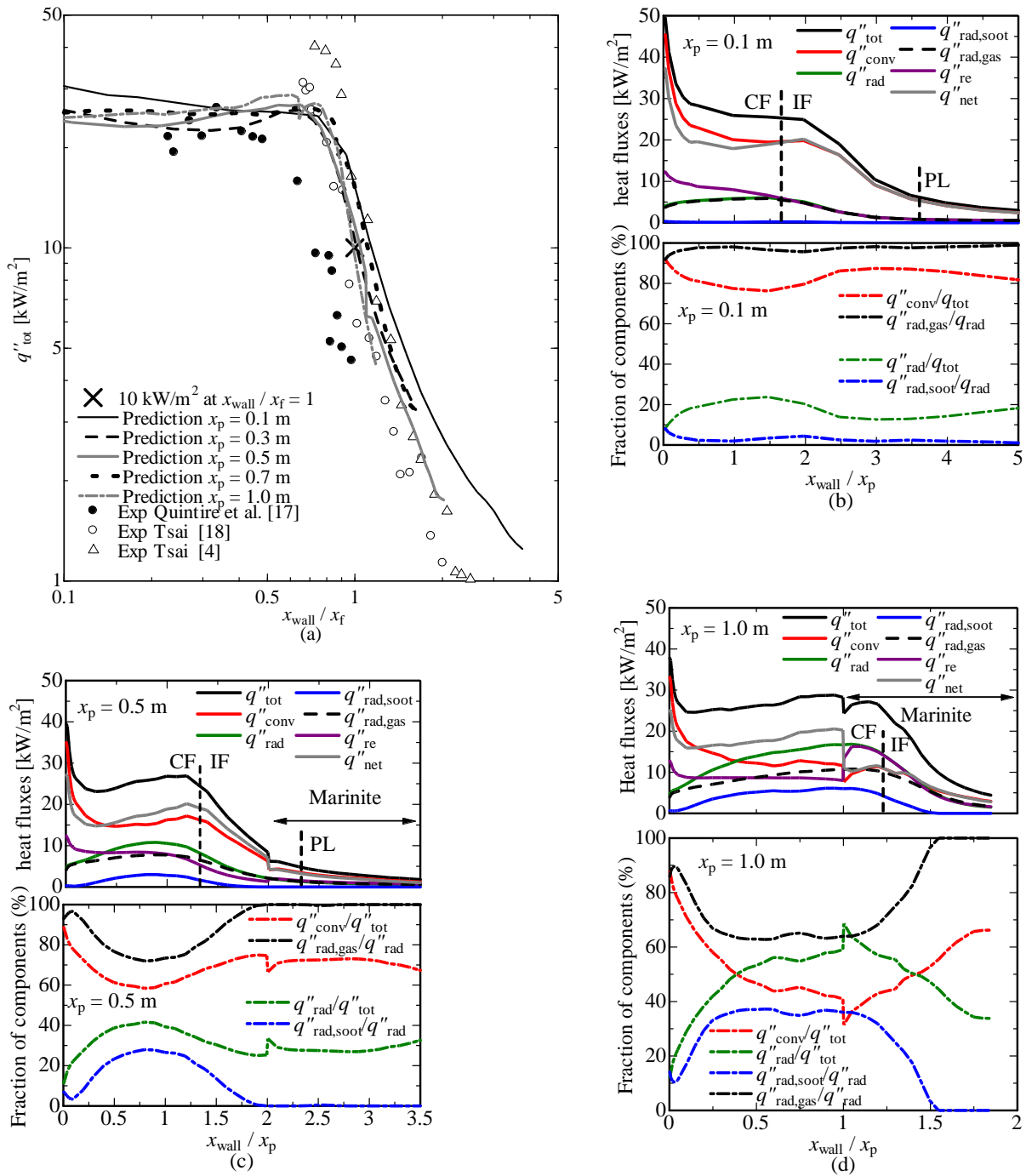


Figure 4 Total heat flux, individual heat fluxes, and fractions of individual components at $x_p = 0.1, 0.5$ and 1.0 m.

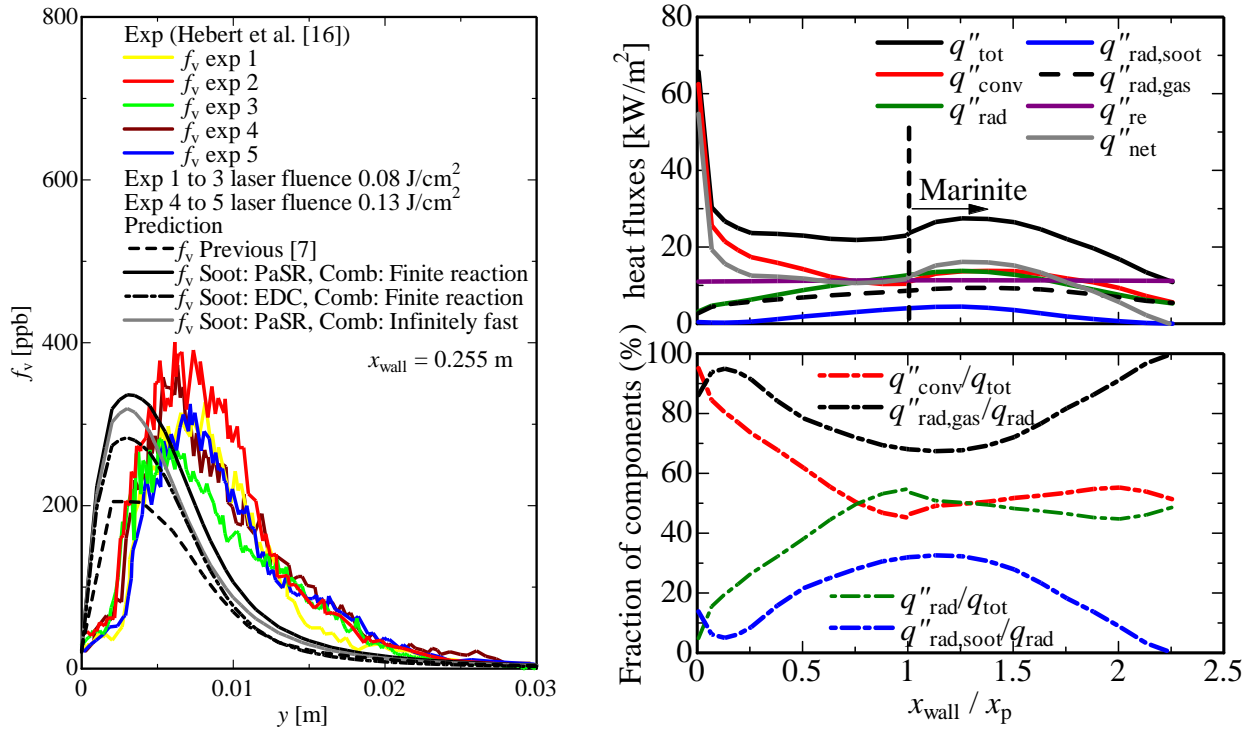


Figure 5 Soot volume fraction f_v (left); heat fluxes and those components (right) for the medium wall fire scenario.

Figure 5 (left) shows that the predicted soot volume fraction f_v is compared with the experiments along with three different combustion and soot oxidation treatments, where ‘Soot: PaSR’ is a soot oxidation rate is computed by Wang et al. model [11], ‘Soot EDC’ is Chen et al.’s model [8], ‘Comb: Finite reaction’ is the combustion model based on a finite reaction rate proposed in this study and ‘Comb: infinitely fast’ is the combustion model based on infinitely fast chemistry [7]. As shown in Fig. 5 (left), the numerical f_v is in reasonably good agreement with the experimental data, indicating that $q''_{\text{rad,soot}}$ is thought to be reliable in Fig. 5 (right). As confirmed in Fig. 4, q''_{tot} was close to the experiments; therefore, a total of q''_{conv} and q''_{rad} is agreed; however their fraction is still not clear. q''_{rad} is estimated as $q''_{\text{rad}} = q''_{\text{rad,gas}} + q''_{\text{rad,soot}}$, where $q''_{\text{rad,gas}}$ is obtained by the WSGGM which is widely used for combustion simulation. Therefore, assuming a reasonable accuracy of $q''_{\text{rad,gas}}$, q''_{rad} is postulated as correct. q''_{tot} is validated in Fig. 4; thus, q''_{conv} is also assumed to be in reasonable agreement with the experimental data.

4 Conclusions

The present work has evaluated a role of respective components of convective and radiative heat transfer fluxes owing to soot and a combustion gas depending on progression of fire spreading. The sound predictions of individual components are of importance for computing flame spreading phenomena.

References

- [1] Orloff L. de Ris J. Markstein GH. (1975). Upward turbulent fire spread and burning of fuel surface. *Proc. Combust. Inst.* 15: 183.
- [2] Liang C. Cheng X. Yang H. Zhang H. Yuen KK. (2016). Experimental study of vertically upward flame spread over polymethyl methacrylate slabs at different altitudes. *Fire Mater.* 40: 472.
- [3] Singh AV. Gollner MJ. (2015) Experimental methodology for estimation of local heat fluxes and burning rates in steady laminar boundary layer diffusion flames, *Combust. Flame* 162: 2214.
- [4] Tsai KC. (2011) Influence of sidewalls on width effects of upward flame spread, *Fire Safety J.* 46: 294–304.
- [5] Ren N. Wang Y. Vilfayeau S. Trouvé A. (2016) Large eddy simulation of vertical turbulent wall fires, *Combust. Flame* 169: 194.
- [6] FM Global, FireFOAM 2.2.x, Available from: <https://github.com/fireFoam-dev/fireFoam-2.2.x>
- [7] Fukumoto K. Wang CJ. Wen JX. (2018). Large eddy simulation of upward flame spread on PMMA walls with a fully coupled fluid-solid approach, *Combust. Flame.* 190: 365
- [8] Chen Z. Wen J. Xu B. Dembele S. (2014) Large eddy simulation of a medium-scale methanol pool fire using the extended eddy dissipation concept. *Int. J. Heat Mass Trans.* 70: 389.
- [9] Fukumoto K. Wang CJ. Wen J. (2019) Large eddy simulation of a syngas jet flame: Effect of preferential diffusion and detailed reaction mechanism. *Energ Fuel.* doi: 10.1021/acs.energyfuels.9b00130
- [10] Fernández-Tarrazo E. Sánchez AL. Liñán AF. Williams A. (2006). A simple one-step chemistry model for partially premixed hydrocarbon combustion, *Combust. Flame* 147 32.
- [11] Wang CJ. Liu HR. Wen JX. (2018). An improved PaSR-based soot model for turbulent fires. *Appl. Therm. Eng.* 129: 1435.
- [12] Tewarson A. (1986). Prediction of fire properties of materials. Part 1: aliphatic and aromatic hydrocarbons and related polymers. National Institute of Standards and Technology. Gaithersburg. MD. Report No. NBS-GCR-86-521.
- [13] Smith TF. Shen ZF. Friedman JN. (1982). Evaluation of coefficients for the weighted sum of gray gases model, *J. Heat Trans.* 104: 602.
- [14] Beard AN. (2010) Flashover and boundary properties. *Fire Saf. J.* 45: 116.
- [15] Poling BE. Prausnitz JM. O’Connell JP. (2001). *The properties of gases and liquids*, 5th ed., McGraw-Hill, U.S.
- [16] Hebert D. Coppalle A. Talbaut M. (2013). 2D soot concentration and burning rate of a vertical PMMA slab using Laser-Induced Incandescence. *Proc. Combust. Inst.* 34: 2575.
- [17] Quintiere J., Harkleroad M., Hasemi Y. (1986). Wall flames and implications for upward flame spread, *Combust Sci and Technol* 48:191.
- [18] Tsai KC. (2009), Width effect on upward flame spread. *Fire Safety J*, 44: 962.